NASA/TM—2007-214428

Experimental Performance Evaluation of a High Speed Permanent Magnet Synchronous Motor and Drive for a Flywheel Application at Different Frequencies

Aleksandr S. Nagorny
Glenn Research Center, Cleveland, Ohio

Ralph H. Jansen
University of Toledo, Toledo, Ohio

M. David Kankam
Glenn Research Center, Cleveland, Ohio

December 2007

NASA STI Program . . . in Profile

Since its founding, NASA has been dedicated to the advancement of aeronautics and space science. The NASA Scientific and Technical Information (STI) program plays a key part in helping NASA maintain this important role.

The NASA STI Program operates under the auspices of the Agency Chief Information Officer. It collects, organizes, provides for archiving, and disseminates NASA's STI. The NASA STI program provides access to the NASA Aeronautics and Space Database and its public interface, the NASA Technical Reports Server, thus providing one of the largest collections of aeronautical and space science STI in the world. Results are published in both non-NASA channels and by NASA in the NASA STI Report Series, which includes the following report types:
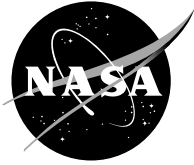
- TECHNICAL PUBLICATION. Reports of completed research or a major significant phase of research that present the results of NASA programs and include extensive data or theoretical analysis. Includes compilations of significant scientific and technical data and information deemed to be of continuing reference value. NASA counterpart of peer-reviewed formal professional papers but has less stringent limitations on manuscript length and extent of graphic presentations.

- TECHNICAL MEMORANDUM. Scientific and technical findings that are preliminary or of specialized interest, e.g., quick release reports, working papers, and bibliographies that contain minimal annotation. Does not contain extensive analysis.

- CONTRACTOR REPORT. Scientific and technical findings by NASA-sponsored contractors and grantees.

- CONFERENCE PUBLICATION. Collected papers from scientific and technical conferences, symposia, seminars, or other meetings sponsored or cosponsored by NASA.

- SPECIAL PUBLICATION. Scientific, technical, or historical information from NASA programs, projects, and missions, often concerned with subjects having substantial public interest.

- TECHNICAL TRANSLATION. English-language translations of foreign scientific and technical material pertinent to NASA's mission.

Specialized services also include creating custom thesauri, building customized databases, organizing and publishing research results.

For more information about the NASA STI program, see the following:

- Access the NASA STI program home page at *http://www.sti.nasa.gov*

- E-mail your question via the Internet to *help@sti.nasa.gov*

- Fax your question to the NASA STI Help Desk at 301–621–0134

- Telephone the NASA STI Help Desk at 301–621–0390

- Write to:
  NASA STI Help Desk
  NASA Center for AeroSpace Information
  7115 Standard Drive
  Hanover, MD 21076–1320

Experimental Performance Evaluation of a High Speed Permanent Magnet Synchronous Motor and Drive for a Flywheel Application at Different Frequencies

Aleksandr S. Nagorny
Glenn Research Center, Cleveland, Ohio

Ralph H. Jansen
University of Toledo, Toledo, Ohio

M. David Kankam
Glenn Research Center, Cleveland, Ohio

National Aeronautics and
Space Administration

Glenn Research Center
Cleveland, Ohio 44135

December 2007

Experimental Performance Evaluation of a High Speed Permanent Magnet Synchronous Motor and Drive for a Flywheel Application at Different Frequencies

Aleksandr S. Nagorny[*]
National Aeronautics and Space Administration
Glenn Research Center
Cleveland, Ohio 44135

Ralph H. Jansen
University of Toledo
Toledo, Ohio 43606–3390

M. David Kankam
National Aeronautics and Space Administration
Glenn Research Center
Cleveland, Ohio 44135

Abstract

This paper presents the results of an experimental performance characterization study of a high speed, permanent magnet motor/generator (M/G) and drive applied to a flywheel module. Unlike the conventional electric machine the flywheel M/G is not a separated unit; its stator and rotor are integrated into a flywheel assembly. The M/G rotor is mounted on a flywheel rotor, which is magnetically levitated and sealed within a vacuum chamber during the operation. Thus, it is not possible to test the M/G using direct load measurements with a dynamometer and torque transducer. Accordingly, a new in-situ testing method had to be developed. The paper describes a new flywheel M/G and drive performance evaluation technique, which allows the estimation of the losses, efficiency and power quality of the flywheel high speed permanent magnet M/G, while working in vacuum, over wide frequency and torque ranges. This method does not require any hardware modification nor any special addition to the test rig. This new measurement technique is useful for high-speed applications, when applying an external load is technically difficult.

I. Introduction

High-speed flywheel system is an energy storage technology, under consideration for use in a variety of applications. Flywheels offer some important advantages over chemical batteries, including higher energy and power densities, longer life, deeper depth of discharge and wider operating temperature range. The energy conversion from electrical to mechanical form (during the charge, or motor, mode) and from the mechanical to electrical form (during the discharge, or generator, mode) occurs in a high frequency permanent magnet motor/generator (M/G) attached to the flywheel rotor. Thus the M/G is a key component of the flywheel energy storage system, and the effectiveness of the energy conversion process mainly depends on the combined efficiency of the M/G and drive. The drive includes an inverter, filters and a control system. For the last several years, a team at the NASA Glenn Research Center (GRC) in Cleveland, Ohio, USA has been working on the development of high efficiency flywheel energy storage technology for space applications. Figure 1 shows the main components of one of GRC's flywheel systems, designated as the G2 module.

The module subsystems include the rotor, magnetic bearings, motor/generator, touchdown bearings, and the housing. The rotor consists of three main parts: the rim, the motor rotor, and the hub. The rim is the main energy storage component made of carbon fiber, using a multi-ring press fit design. The M/G is a two-pole surface mounted permanent magnet synchronous motor, purchased from a commercial vender. The rim and motor rotor are mounted on the hub which is made of titanium. Magnetic bearings are used for the low-loss suspension of the rotor. The M/G is used to convert electrical energy into rotational kinetic energy of the flywheel rotor during the charge (or motor) mode, and from rotational kinetic energy to electrical energy during the discharge (or generator) mode. The touchdown bearings are designed to capture the rotor in the event of a magnetic bearing failure and, also, to support the rotor when the active magnetic bearings are turned off. The module housing supports the stationary parts of the flywheel system, including the motor/generator and magnetic bearing stators, the position sensors, and the touchdown bearings. Additionally the housing acts as a vacuum chamber, allowing the rotor to operate with minimal windage loss.

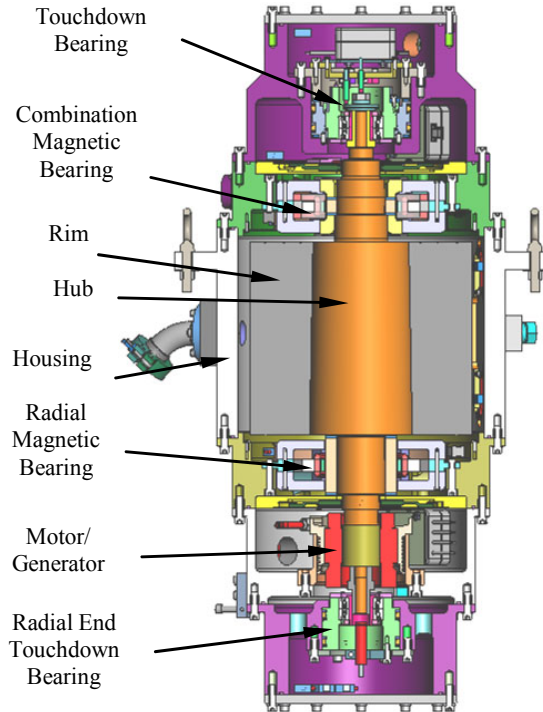[*]National Research Council Fellow

Figure 1.—NASA GRC G2 Flywheel
module cross section.

During normal operation, the G2 flywheel accelerates from its minimum speed (20 krpm) to its maximum speed (60 krpm) while in the charge (motor) mode, and decelerates from the maximum to the minimum speed while operating in the discharge (generator) mode. In a satellite application, the charging power is provided by a solar array during solar insolation. When the satellite is shadowed by the planet, the flywheel discharges to provide power to the spacecraft systems and payloads (ref. 1). Thus, the efficiency of the M/G and drive should ideally be determined over a broad range of operating frequency and torque.

Since the flywheel housing is a sealed vacuum chamber and its rotor levitates in a magnetic field during the operation, it is not possible to test the flywheel M/G under direct load as is typically done using a dynamometer with torque and speed transducers. Building a special load test fixture inside the vacuum chamber may be possible, but it is technically difficult and expensive. However, the knowledge of the M/G and inverter efficiencies over broad operating frequency and load ranges is essential for the selection and improvement of the drive components; therefore, another test method was required. This paper presents a relatively simple in-situ efficiency estimation method for the M/G and drive. The method does not require hardware modification or additional test fixtures. The results of the experimental performance evaluation of the G2 module are, also, presented.

II. Power and Losses in Flywheel M/G and Drive

The power balance equation of the flywheel M/G in a motor mode is:

$$P_{DC} = P_{M/G} + P_{inv} \qquad (1)$$

where P_{DC} the electrical power coming into the inverter from the DC link, $P_{M/G}$ is the output power of the inverter and P_{inv} represents power losses in the drive. The drive losses include the switching losses and conduction losses in the inverter and filters. The efficiency of the drive in the motor mode can be defined as:

$$\eta_{inv} = P_{M/G} / P_{DC} \qquad (2)$$

The power equation for the M/G in the motor mode can be described as

$$P_{M/G} = P_{out} + \sum P \qquad (3)$$

where the P_{out} is the mechanical output power of the M/G and $\sum P$ is the sum of the M/G losses. The $\sum P$ losses of the flywheel M/G can be divided into two major groups: current losses and rotational losses. The current loss is caused by the stator winding current and, for a high-speed flywheel M/G, it also includes the additional losses caused by the high frequency skin- and proximity effects. Unlike the current loss in low frequency machines, this current loss cannot be determined by using the I^2R formula (where R is the measured stator DC resistance) without a significant error. The rotational loss of the flywheel includes the M/G stator iron loss, the M/G rotor loss inclusive of eddy current losses induced in the permanent magnets and the solid rotor, the magnetic bearing losses, and the windage loss caused by residual air pressure in the flywheel module (the vacuum inside the chamber is not ideal). The efficiency of the M/G is:

$$\eta_{M/G} = P_{out} / P_{M/G} \qquad (4)$$

and the total efficiency of the flywheel drive is:

$$\eta_{tot} = \eta_{inv}\eta_{M/G} \qquad (5)$$

III. Experimental Efficiency Determination and Results

This study was performed on the G2 flywheel module. A simplified schematic of the M/G and drive configuration is depicted in figure 2. The motor control algorithm uses a sensorless field oriented method. The position and speed
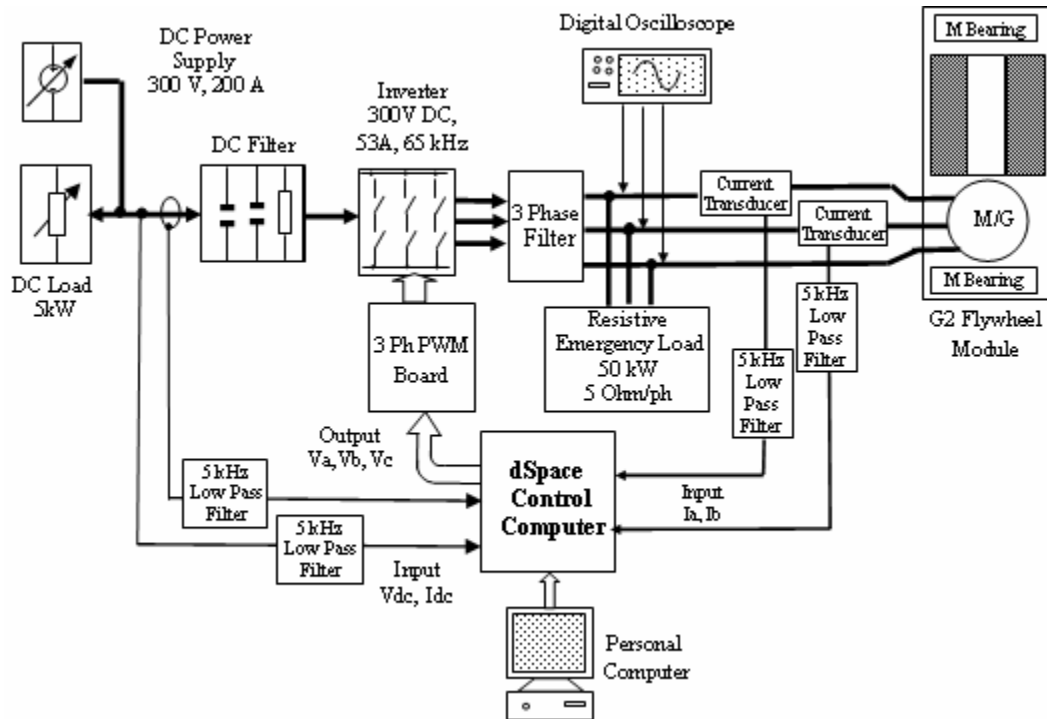
Figure 2.—Flywheel G2 Motor/Generator testing setup.

estimates are made by the signal injection technique in the speed range from 0 to 1200 rpm, and by the back EMF technique from 1200 to 40000 rpm (ref. 2). The drive control was implemented using rapid prototype hardware with a Central Processor Unit (CPU) and input and output interface boards and a PC based graphical user interface. The analog motor control signals from the controller are converted to switch states by using a special PWM circuit. This circuit includes a comparator, a triangular wave generator and a gate driver that sends signals to a commercially available 3-phase inverter driving the flywheel motor. A commercial power supply is used as the DC power source for the inverter. Feedback signals for the controller include two motor phase currents, the DC bus current, and the DC bus voltage.

A custom high speed synchronous permanent magnet motor was built for this flywheel module. The motor parameters are given in table 1.

TABLE I.—M/G parameters

Output power, kW	3
Rated Voltage at highest speed rms, V	80
Number of poles	2
Speed range, krpm	6-60
Frequency at highest speed, Hz	1000
Type of the rotor	Surface Mounted
Type of the cooling system	Water

The following three types of tests were performed to determine the M/G and drive losses: locked rotor tests, no-

load tests, and constant current tests. Each group of tests was performed at different current frequencies.

A common technique was applied for all three test types. The control system described above was used to command M/G current RMS values between 2 and 20A, at frequencies between 0 and 1000 Hz. During the tests, the instantaneous values of DC bus voltages and currents and phase voltages and currents as functions of time were captured and recorded using an isolated multi-input digital oscilloscope.

The following analysis was applied to the test data in order to determine the DC bus and motor power. The electrical power coming into the inverter from the DC link is

$$P_{DC} = V_{DC} \cdot I_{DC} \tag{6}$$

where V_{DC} and I_{DC} are the values of DC bus voltage and current.

The instantaneous value of the power coming from the inverter to the M/G is

$$P_{M/G} = v_a \cdot i_a + v_b \cdot i_b + v_c \cdot i_c \tag{7}$$

where v_a, v_b, v_c and i_a, i_b, i_c are respectively the instantaneous AC values of M/G phase voltages and currents.

The locked rotor tests were used to determine the M/G current loss including the high frequency component due to the skin and proximity effects. The tests were conducted for a number of stator current fundamental frequency values,
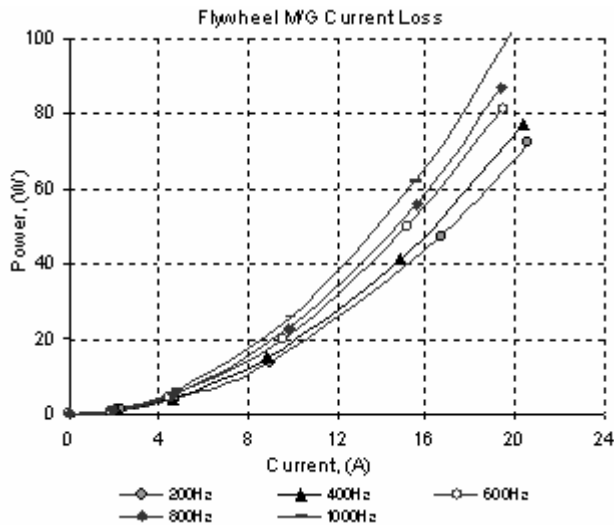
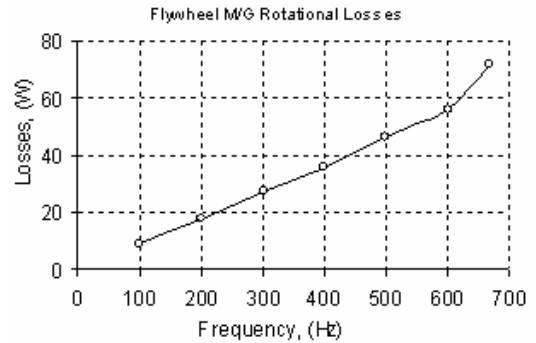Figure 3.—The flywheel M/G current loss
for different frequencies.

Figure 4.—The flywheel M/G rotational
losses at different frequencies.

Figure 5.—The flywheel rotational losses
measured from the spin down test.

ranging from 0 to 1000 Hz. For each frequency, the measurements were taken by varying the stator current values from zero to the rated value. The current loss of the M/G as a function of current and frequency is depicted in figure3

The high-frequency skin- and proximity effects can be evaluated using the curves shown in figure 3. These effects depend on the particular motor geometry and wire size. For the tested M/G, increasing the drive frequency from 200 to 1000 Hz increases the current loss by approximately 40 percent.

The rotational losses of the M/G were determined by performing a series of no-load tests. The no-load tests were conducted for the same frequency points which were used in the locked rotor tests. For each test frequency, the minimum value of the current required to maintain speed was found, and the test data was recorded. In this condition, the power required by the M/G (no-load power) is equal to the sum of the current loss and the rotational losses. Therefore, at each frequency the rotational losses can be determined by subtracting the corresponding current loss (found during the locked rotor tests) from the no-load power. The results are presented in figure 4.

It should be mentioned that this test is relatively difficult to perform, because the current controller is less accurate at low current, and the total harmonic distortion (THD) at low current is relatively high.

Another way to determine the M/G rotational losses is by performing a spin-down test. During this test, the flywheel is accelerated up to the speed corresponding to the maximum test frequency value, and then the M/G is disconnected from the power source and the load. As the flywheel decelerates, the rotational speed is recorded as a function of time. The kinetic energy of the flywheel rotor can be calculated as

$$E_{fl} = \frac{1}{2} J \cdot \varpi^2 \qquad (8)$$
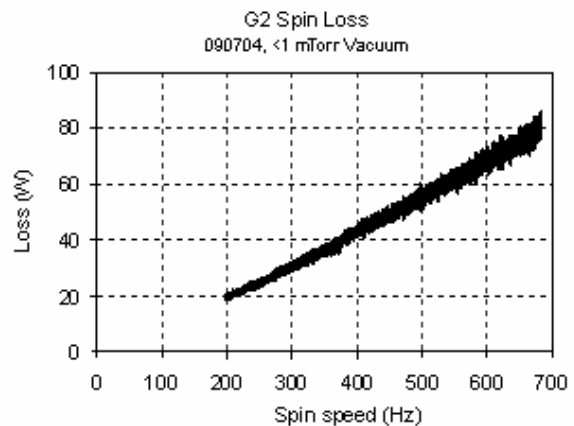
where J-is the moment of inertia of the flywheel rotor and ϖ-is the angular velocity. The rotational losses can be found as $\dfrac{dE_{fl}}{dt}$. These measurements were made to confirm the no-load tests data. The results are depicted in figure 5.

For the constant current measurements, a test matrix was selected which included frequency measurement points from 100 to 600 Hz in 100 Hz increments, as well as a measurement at 667 Hz, at rms current values from 2 to 20 A (rated point). Using this technique, P_{DC} and $P_{M/G}$ were determined for all tests, and the inverter and filter losses were found using equation (1). Then, the mechanical output power of the M/G P_{out} could be determined by subtracting the sum of the current loss and rotational loss found in the locked rotor and no-load tests from $P_{M/G}$. The phase voltage, current and power waveforms at 667 Hz are plotted in figure 6. The power factor for each phase can be determined from the electrical angle between voltage and current. The M/G and drive efficiency values were determined from the equations (2), (4) and (5). Figure 7 shows the results of the efficiency estimation as a function of the phase current, and figure 8 illustrates the M/G, inverter and drive efficiency as a function

of drive frequency. It should be noted that the efficiency is lower at low speed (frequency) because the output power is small in relation to the bearing and windage losses. These graphs also demonstrate that beyond 300 Hz, the efficiency begins to decrease because of high frequency losses.

As mentioned above, a field-oriented control algorithm is used for the motor control. This algorithm keeps the current vector positioned to provide maximum torque to current ratio (ref. 2). Therefore, the angle between the stator current vector and the rotor pole field (the torque angle) is a constant value.

The M/G power factor is illustrated in figure 9 as a function of the stator current and frequency. Note that the power factor is close to unity throughout most of the current range at 100 Hz, and that power factor significantly decreases with frequency.

The M/G torque is plotted as a function of the stator current and frequency in figure 10. The relationship between torque and drive current is linear for this type of control, as expected. The current component $I_d = 0$, so that at every point $I = Iq$. From the graph, we see that the slopes of the lines (torque constants) are decreasing with the frequency, which due to the influence of high frequency losses.
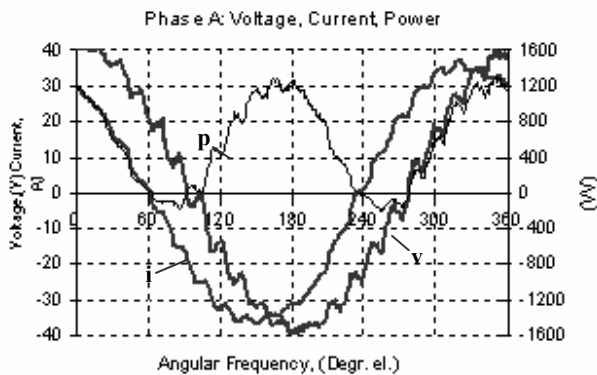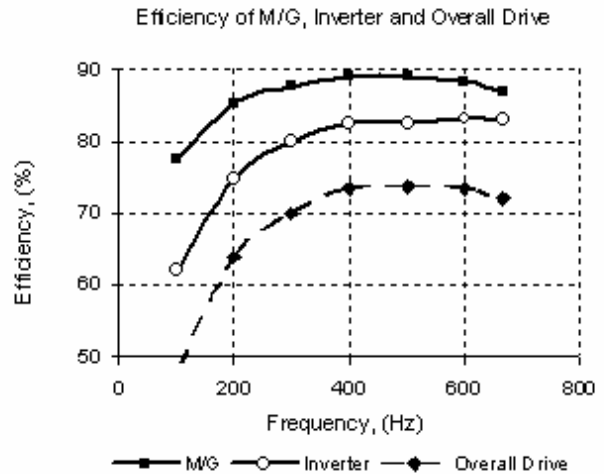

Figure 8.—M/G, inverter and drive efficiency as a function of frequency.

Figure 9.—M/G power factor as a function of current and frequency.

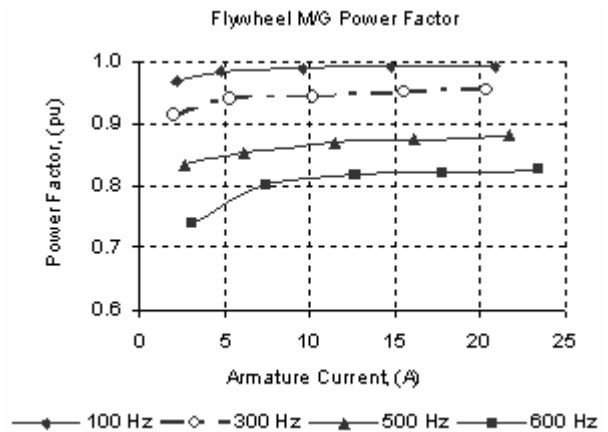Figure 6.—The M/G phase voltage, current and power waveforms at 666.7 Hz.

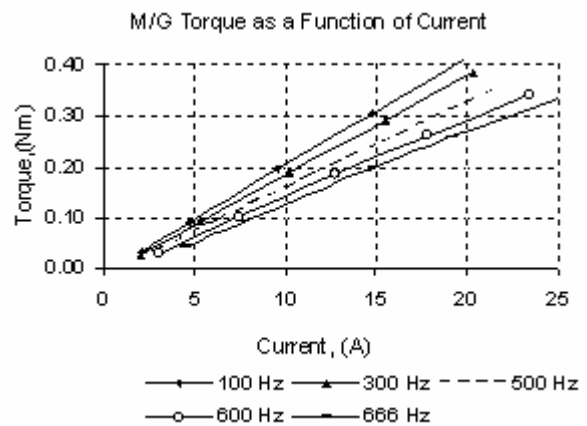Figure 7.—The M/G efficiency as a function of a phase current.

Figure 10.—The M/G torque as a function of current and frequency.

The time harmonics spectrum is an important indicator of controller performance and inverter output power quality. It can be estimated using the Total Harmonic Distortion (THD) parameter. In our case, the THD was determined for the first 12 time harmonics of the phase current using the expression:

$$THD = \frac{\sqrt{\left(I_{m2}^2 + I_{m3}^2 + \cdots \div I_{m12}^2\right)}}{I_{m1}} \cdot 100\% \qquad (9)$$

where: $I_{m1}, I_{m3\cdots}$ are the phase current harmonic amplitudes.

The THD for the M/G at three different frequencies is presented in figure 11. The THD at low currents exceeds 10 percent, but drops to 5 to 7 percent at currents above 7A.
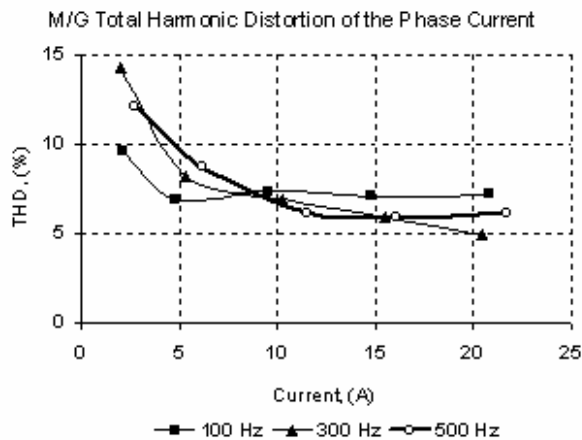

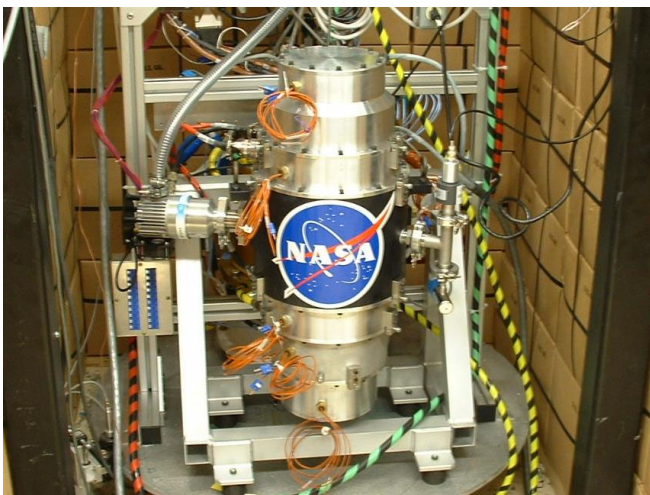Figure 11.—The M/G total harmonic distortion (THD) of the phase current.

Figure 12.—NASA GRC G2 flywheel module.

IV. Conclusions

This paper describes an in-situ flywheel motor and drive efficiency measurement technique, and presents experimental results on the NASA Glenn Research Center G2 flywheel module. This measurement technique is useful in high speed applications where the addition of external loads is difficult.

Losses, efficiency, and power factor were determined for the G2 flywheel. The flywheel M/G winding current losses increase with the frequency due to the skin- and proximity-effects. The maximum of the motor efficiency was found approximately at 300 Hz operating frequency. Bearing losses were important at low speed and high frequency losses began to be apparent over 300 Hz.

A power factor study, as a function of load and frequency, was performed. The results show that with the field oriented control algorithm used to maximize the torque to current ratio, the power factor decreases with the increasing of operating frequency.

The M/G torque as a function of the stator current and frequency was also studied. The results show that the dependency between the torque and the stator current is linear, and that the torque constants decrease with increased frequency, which might be explained by the influence of high frequency losses.

References

1. A.S. Nagorny, N.V. Dravid, R.H. Jansen, B.H. Kenny "Design Aspects of a High Speed Permanent Magnet Synchronous Motor/Generator for Flywheel Applications," *International Electric Machines and Drive Conference (IEMDC 05)* San Antonio, Texas, May 2005
2. B.H. Kenny, P.E. Kascak, "Sensorless Control of Permanent Magnet Machine for NASA Flywheel Technology Development," *37th Annual IECEC*, Washington DC., July 28-August 2, 2002.

1. REPORT DATE (DD-MM-YYYY) 01-12-2007	2. REPORT TYPE Technical Memorandum	3. DATES COVERED (From - To)

4. TITLE AND SUBTITLE Experimental Performance Evaluation of a High Speed Permanent Magnet Synchronous Motor and Drive for a Flywheel Application at Different Frequencies	5a. CONTRACT NUMBER
	5b. GRANT NUMBER
	5c. PROGRAM ELEMENT NUMBER
6. AUTHOR(S) Nagorny, Aleksandr, S.; Jansen, Ralph, H.; Kankam, M., David	5d. PROJECT NUMBER
	5e. TASK NUMBER
	5f. WORK UNIT NUMBER WBS-22-755-922-20

7. PERFORMING ORGANIZATION NAME(S) AND ADDRESS(ES) National Aeronautics and Space Administration John H. Glenn Research Center at Lewis Field Cleveland, Ohio 44135-3191	8. PERFORMING ORGANIZATION REPORT NUMBER E-15705

9. SPONSORING/MONITORING AGENCY NAME(S) AND ADDRESS(ES) National Aeronautics and Space Administration Washington, DC 20546-0001	10. SPONSORING/MONITORS ACRONYM(S) NASA
	11. SPONSORING/MONITORING REPORT NUMBER NASA/TM-2007-214428

12. DISTRIBUTION/AVAILABILITY STATEMENT
Unclassified-Unlimited
Subject Categories: 20, 31, and 33
Available electronically at http://gltrs.grc.nasa.gov
This publication is available from the NASA Center for AeroSpace Information, 301-621-0390

13. SUPPLEMENTARY NOTES

14. ABSTRACT
This paper presents the results of an experimental performance characterization study of a high speed, permanent magnet motor/generator (M/G) and drive applied to a flywheel module. Unlike the conventional electric machine the flywheel M/G is not a separated unit; its stator and rotor are integrated into a flywheel assembly. The M/G rotor is mounted on a flywheel rotor, which is magnetically levitated and sealed within a vacuum chamber during the operation. Thus, it is not possible to test the M/G using direct load measurements with a dynamometer and torque transducer. Accordingly, a new in-situ testing method had to be developed. The paper describes a new flywheel M/G and drive performance evaluation technique, which allows the estimation of the losses, efficiency and power quality of the flywheel high speed permanent magnet M/G, while working in vacuum, over wide frequency and torque ranges. This method does not require any hardware modification nor any special addition to the test rig. This new measurement technique is useful for high-speed applications, when applying an external load is technically difficult.

15. SUBJECT TERMS
Flywheels; Efficiency; Losses; Motor/Generator

16. SECURITY CLASSIFICATION OF:			17. LIMITATION OF ABSTRACT	18. NUMBER OF PAGES	19a. NAME OF RESPONSIBLE PERSON STI Help Desk (email:help@sti.nasa.gov)
a. REPORT U	b. ABSTRACT U	c. THIS PAGE U	UU	12	19b. TELEPHONE NUMBER (include area code) 301-621-0390